Article

Discovery Medicine 2023; 35(179): 956–964
https://doi.org/10.24976/Discov.Med.202335179.91

Noggin Protein can Induce the Differentiation of Rat Bone Marrow Mesenchymal Stem Cells to Neurons and Repair Spinal Cord Injury

Wei Liu[1,†], Fang Luo[2,†], Hongwei Wu[1], Huimin Li[1], Guangchao Bai[1,*]

[1]Department of Orthopaedics, Fourth Affiliated Hospital of Zhejiang University School of Medicine, 322000 Yiwu, Zhejiang, China
[2]Department of Emergency Medicine, Yiwu Central Hospital, 322000 Yiwu, Zhejiang, China
*Correspondence: 8018140@zju.edu.cn (Guangchao Bai)
[†]These authors contributed equally.
Published: 1 December 2023

Background: Addressing spinal cord injury (SCI) through stem cell therapy is currently at the forefront of medical research despite its complexity. In this study, we investigated the potential of the Noggin protein in promoting the differentiation of rat bone marrow mesenchymal stem cells (BMSCs) into neuronal cells. We transplanted induced cells into a rat model with spinal cord injury. This exploration proposes an innovative perspective on stem cell therapies for spinal cord injuries.
Methods: Rat BMSCs were isolated utilizing the bone marrow cell apposition method; The multidirectional differentiation of rat BMSCs was identified by lipid induction and osteogenic induction; Rat BMSCs were induced by different concentrations of Noggin protein and different induction times; Nissel staining was used to identify the induced neuronal-like cells; The expression of synaptic protein I (SYN1), glial fibrillary acidic protein (GFAP), and neurofilament protein 200 (NF200) in neuron-like cells was detected by immunofluorescence assay. Rats were randomly divided into a control group and a neuron-like cell group; A rat spinal cord injury model was produced, and neuron-like cells obtained from induction were transplanted into the rat's SCI. The recovery of the rats' hind limbs' motor function was detected by the Basso, Beattie, and Bresnahan (BBB) scores, and the changes in the expression of NF200 mRNA at the spinal cord injury were detected by quantitative real time polymerase chain reaction (qRT-PCR).
Results: Our cultured rat BMSCs had a long spindle-shaped morphology and stained positively for oil red O after lipogenic induction and modified alizarin red S after osteogenic induction. Nissel staining of cells obtained from rat BMSCs induced by Noggin protein was positive. Immunofluorescence results showed that the induced neuronal-like cells positively expressed NF200 and SYN1, and negatively expressed GFAP. After local transplantation of induced neuronal-like cells in the rat SCI model, the BBB scores in the neuron-like cell group were higher than those in the control group at 1 w, 2 w, and 4 w, with statistically different results ($p < 0.05$). According to qRT-PCR results, NF200 at the spinal cord injury in the neuron-like cell group was higher than that in the control group at 12 h, 3 d, 1 w, 2 w, and 4 w, with statistically significant differences in results ($p < 0.05$).
Conclusions: Our findings indicate that Noggin protein effectively facilitates the differentiation of rat BMSCs into neuronal cells, highlighting its potential as a therapeutic agent for repairing spinal cord injuries. This study elucidates a promising avenue in stem cell research, contributing a novel approach to regenerative strategies for spinal cord injuries.

Keywords: Noggin; bone marrow mesenchymal stem cells; neuron; spinal cord injury; rat; neural induction

Introduction

Addressing spinal cord injuries (SCI) remains a significant medical challenge and a focus of contemporary research [1–3]. Although pharmacological and surgical interventions can mitigate spinal cord edema and restore spinal stability, they fall short of resolving local neuronal necrosis and axonal disconnections [4,5]. The current research on stem cell therapy for spinal cord injury mainly involves the use of growth factors, stem cells and biomaterial scaffolds to construct tissue-engineered materials, which are further transplanted to the spinal cord injury for the treatment of spinal cord injury. So that the safety and validity of tissue-engineered methods have not yet been effectively demonstrated [6]. The discrepancies in the microenvironment underscore the importance and relevance of exploring localized transplantation of induced neuronal cells directly at the injury site, which is an interesting exploration.

Currently, the most commonly used stem cells in tissue engineering include bone marrow mesenchymal stem cells (BMSCs), embryonic stem cells (ESCs), human umbilical cord blood mesenchymal stem cells, and neural stem cells. BMSCs, in particular, are the focus of extensive research because of their accessibility, cultivability and min-

imized risk of immune rejection [7]. Noggin is a secreted protein with a molecular weight of 26 kD and a hydrophobic C-terminal. It was first isolated from Xenopus laevis embryos in 1992 by Harland and William Smith of the University of California. Noggin derived its name from the noted enlargement of the head following mRNA injections in Xenopus laevis embryos [8]. Subsequent studies illuminated Noggin protein's role in fostering neurogenesis. Notably, Farrukh's research [9] unveiled that Noggin proteins modulate the neural stem cell differentiation balance between glial cells and neurons by counteracting bone morphogenetic protein (BMP) 2/4. This elucidated that while BMP augments glial cell differentiation and suppresses neuron generation, Noggin promotes neuronal formation, restrains astrocyte differentiation, and encourages axonal regeneration and myelin basic protein production.

Therefore, in the present study, we utilized Noggin protein to induce the differentiation of BMSCs into neurons. These induced cells were subsequently transplanted into the SCI site in rats to assess their potential for spinal cord repair. This study provides a theoretical foundation for employing Noggin protein in treating SCI. It enriches the repertoire of biological treatments and stem cell therapies available for SCI, offering a novel perspective and approach in the therapeutic landscape of spinal cord injuries.

Experimental Methods and Design

Main Reagents

Noggin protein (PEPROTECH, HY-P700286-246064, Cranbury, NJ, USA); Dulbecco's Modification of Eagle's Medium (DMEM, GIBCO, 11995040, Waltham, MA, USA); Phosphate Buffered Saline (PBS, GIBCO, AM9625, Waltham, MA, USA); Fetal Bovine Serum (FBS, GIBCO, 16140071, Waltham, MA, USA); Double antibody (GIBCO, 15140122, Waltham, MA, USA); Mycoplasma Routine PCR Kit (Beyotime Biotechnology, C0301S, Shanghai, China); Rat BMSCs osteogenesis-induced differentiation complete medium (Cyagen, RASMX-90021, Guangzhou, Guangdong, China); Oil Red O staining kit (Amresco, S0034, Sussex, NJ, USA); Calcium Salt Staining Kit (Solarbio, GL0910-ZES, Beijing, China); Basic Fibroblast Growth Factor (bFGF, GIBCO, 13256029, Waltham, MA, USA); Nissel Staining Kit (Solarbio, G1432, Beijing, China); Bovine Serum Albumin (BSA, GIBCO, 16260-037, Waltham, MA, USA); Quantitative real time polymerase chain reaction (qRT-PCR) Kit (TAKARA, 9108, Tokyo, Japan); Mouse Monoclonal neurofilament protein 200 (NF200), glial fibrillary acidic protein (GFAP), synaptic protein I (SYN1) Antibody (Abbiotec, A10871, San Diego, CA, USA); Sheep anti-mouse secondary antibody (Abbiotec, A10446, San Diego, CA, USA).

Main Instruments

Fluorescence microscope (Carl Zeiss, Oberkochen, Battenwürttemberg, Germany); Enzyme-linked immunoassay detector (Thermo Fisher Scientific, Waltham, MA, USA); –80 ℃ low-temperature refrigerator (Thermo Fisher Scientific, Waltham, MA, USA); Ultra-clean bench (Thermo Fisher Scientific, Waltham, MA, USA); CO_2 incubator (Thermo Fisher Scientific, Waltham, MA, USA); Real-time incubator (Thermo Fisher Scientific, Waltham, MA, USA); Real-time immunoassay (Thermo Fisher Scientific, Waltham, MA, USA); qRT-PCR instrument (Roche, Basel, Switzerland); Nucleic acid protein quantification instrument (Invitrogen, Shanghai, China).

Extraction and Cultivation of Rat BMSCs

Two Sprague Dawley (SD) rats (male, 4 weeks old), weighing about 90 g, were procured from the Experimental Animal Center of Zhejiang University and anesthetized by intraperitoneal injection of 1% sodium pentobarbital (100 mg/kg) and euthanized via by cervical dislocation. The femur and tibia were subsequently isolated using a sharp blade.

The extracted femur and tibia were transferred to an ultra-clean workbench, and the ends of the bones were carefully cut to expose the marrow cavity. The bone marrow cavity was flushed with DMEM using a 2.5 mL syringe until clear, collecting the cell suspension. Cells were then inoculated into 25 cm^2 flasks at a density of 1×10^7 cells/mL and cultivated under the conditions of 37 °C, 5% CO_2, and saturated humidity.

89% DMEM + 10% FBS + 1% double antibody was used to prepare a complete cell culture medium. After 48 hours of culture, half of the medium was exchanged, followed by full medium exchange every 3 days. At cellular confluency at about 80%, cells were passaged at a 1:2 ratio.

Cells obtained in culture were checked for mycoplasma using the Mycoplasma Routine PCR Kit, and subsequent experiments were performed after determining the absence of mycoplasma contamination.

Lipogenic Induction and Oil Red O Staining of BMSCs

Lipogenic induction: Rat BMSCs obtained from the above culture were taken for subsequent experiments. Third-generation rat BMSCs were inoculated into 6-well plates at a density of 2×10^5 units/well. Cultured for 24 hours and then changed to lipogenic induction medium (94.498% DMEM + 0.002% indomethacin + 4% FBS + 0.1% insulin + 0.4% Dexamethasone + 1% double antibody). The solution was changed every three days, and after 28 days of induction, oil red O staining was performed.

Oil red O staining: After discarding the induction solution, the cells were washed twice with PBS; Then after adding the staining solution and discarding the staining so-

lution after 15 minutes, the cells were washed twice with PBS, washed 2 times with pure water, and placed under the microscope.

BMSCs Osteogenic Induction and Modified Alizarin Red S Staining

For osteogenic induction, third-generation BMSCs were prepared and seeded into 6-well plates, precoated with 0.1% gelatin, at 2×10^5 cells/well density. After 24 hours of incubation, the culture medium was replaced with an osteogenic induction solution, with subsequent full medium replacement every three days. The cell morphology was observed under an inverted phase-contrast microscope. After 14 days of induction, cells underwent modified alizarin red S staining for osteoblast identification.

For the alizarin red S staining procedure, the induction medium was discarded, and cells were washed twice with PBS, followed by fixation with 10% formaldehyde for 15 minutes at room temperature. After fixation, cells were washed twice with PBS and stained with 40 mM alizarin red staining solution, with an incubation period of 20 minutes at room temperature with slight agitation. After staining, unbound dye was removed, cells were rinsed by PBS with agitation period of 5 minutes four times, and any excess PBS was carefully discarded. Finally, cells were observed, photographed, and documented under an inverted microscope.

Cell Grouping, Induction and Nissel Staining for Identification

Third-passage rat BMSCs were randomly divided into 5 groups: 25 ng/mL, 50 ng/mL, 75 ng/mL, 100 ng/mL Noggin groups, and a control group. The culture solution for the control group was 90% DMEM + 10% FBS and for the induction group was 25, 50, 75, and 100 ng/mL Noggin + 90% DMEM + 10% FBS.

A six-well plate, precoated with 50 ug/mL polylysine, was prepared, and cells were inoculated at a density of 2×10^5 cells/well, with a complete culture medium added to each well. After 24 hours of culture, the medium was replaced with a pre-induction medium, followed by an induction medium corresponding to each group after 24 hours of pre-induction. Subsequently, Nissel staining was conducted after 1 h, 2 h, 4 h, and 6 h of induction.

For Nissel staining, the induction medium was removed from each group, and the cells were fixed with 4% paraformaldehyde at room temperature for 10 minutes. The cells were then rinsed twice with distilled water and stained with Nissel staining solution for 10 minutes at room temperature. After staining, cells were washed with distilled water and ethanol, followed by observation and imaging under a microscope. The positive rate was analyzed using Image Pro Plus 6.0 software (Media Cybernetics, Rockville, MD, USA), and the optimal concentration group and time point were selected for subsequent experiments based on the highest positive rate.

Immunofluorescence Detection of SYN1, NF200, and GFAP Protein Expression in Neuron-Like Cells

Cells from the control and the 75 ng/mL Noggin group underwent immunofluorescence testing after 2 hours of induction. The induction medium was discarded, and cells were rinsed with PBS twice and fixed with 4% paraformaldehyde for 30 minutes at 4 °C, followed by 3% H_2O_2 for 30 minutes at room temperature and 5% BSA for 20 minutes at room temperature. Excess liquid was removed, incubated with the primary antibody (dilution ratio of 1:100), kept overnight at 4 °C, rewarmed at 37 °C for 45 minutes, incubated with the secondary antibody (dilution ratio of 1:50) for 30 minutes, and incubated at room temperature for 20 minutes in the dark. Following antibody incubation, cells were observed under a fluorescence microscope to detect SYN1, NF200, and GFAP protein expression in neuron-like cells.

Modeling of Rat Spinal Cord Injury

Thirty SD rats were randomly divided into neuron-like cell group and control group, with 15 rats in each group, and 5 time points for testing, with 3 rats in each group for each time point. The SD rats (4 weeks old, weighing about 90 g) used in the experiment were purchased from the Experimental Animal Center of Zhejiang University.

Rats were anesthetized by intraperitoneal injection of 1% sodium pentobarbital (100 mg/kg). The operative area was sterilized with iodophor, after which the 10th thoracic vertebral spinal cord was exposed with a scalpel, and the 10th thoracic vertebral segment of the spinal cord of the rats was further transected with a scalpel.

Criteria for successful SCI modeling: Severed spinal cord in the injured area, convulsively shook tails, retracted and fluttered body, and slowly paralyzed hindlimbs [10].

Preparation of transplanted cells: BMSCs were induced with 75 ng/mL Noggin for 2 hours. The cells were then digested with trypsin, and the cell density was adjusted to 1×10^6/mL for later use.

100 uL of cell suspension was injected into the spinal cord injury in the neuron-like cell group, and the control group was injected with the same volume of saline. The incision was sutured layer by layer, and the rats were raised in a single cage after modeling and then squeezed the bladder 3 times a day to assist in urination. The rats were able to eat and drink.

Basso, Beattie, and Bresnahan (BBB) Score Detection of the Recovery of Hindlimbs Motor Function of Each Group

Hindlimb recovery of rats in each group was assessed using the BBB score at 12 hours, 3 days, 1 week, 2 weeks, and 4 weeks after modeling. Score definition: 0–7 points for the motion of the hindlimbs; 0–6 points for the gait and coordination in motion; 0–8 points for the fine movement of the hindlimbs, with a full score of 21 points [11].

qRT-PCR Detection of the Relative Expression of NF200 mRNA at SCI in Each Group

The BBB scored rats in each group and then injected intraperitoneally with 1% pentobarbital sodium (100 mg/kg) and subsequently executed by cervical dislocation method, the spinal cord specimens were taken along the original incision and ground well for RNA extraction with chloroform. A one-step reverse transcription PCR kit was used to obtain cDNA, and a 20 mL PCR system was used for fluorescence quantification, with Glyceraldehyde-3-Phosphate Dehydrogenase (GAPDH) as an internal reference. NF200 primer sequences (F: 5′-GATGGCATTGGACATTGAGA-3′, R: 5′-GAGAGTAGCCGCTGGTTATG-3′), internal reference sequences (F: 5′-CTGGTCATCAATGGGAAAC-3′, R: 5′-CAAAGTTGTCATGGATG-3′).

The expression of NF200 mRNA in each group cells was calculated according to the following formula: $\Delta\Delta$Ct = sample (target gene Ct value – internal reference Ct value) – control (target gene Ct value – internal reference Ct value); The relative expression of target gene Y = $2^{-\Delta\Delta Ct}$ (multiples relative to the control group).

Statistical Analysis

We used the SPSS 26.0 statistical software (IBM, New York, NY, USA) for statistical analysis, and the measurement was expressed as $\bar{x} \pm$ s. Mean comparison between multiple groups was performed by Analysis of Variance (ANOVA) followed by SNK-q test, comparisons between the two groups were made using the independent samples *t*-test, $p < 0.05$ indicates the difference was statistically significant.

Results

BMSCs Isolation, Culture, and Purification

Given the pivotal role that BMSCs play in various regenerative therapies due to their multipotency and capacity for self-renewal, understanding the intricacies of their isolation, culture, and purification was crucial. This process ensures a consistent and viable cell population for subsequent experimental procedures. The morphology and proliferation of cells were meticulously observed post-inoculation to assess the effectiveness and uniformity of the culture and purification process.

Three days after the inoculation of bone marrow cells, a minor proportion of cells exhibited adherence to the wall and showed noticeable growth. Subsequent media changes and passages led to a reduction in the number of parenchymal cells. By the third generation, a uniform fusiform cell morphology was observed, exhibiting aggregated growth (Fig. 1).

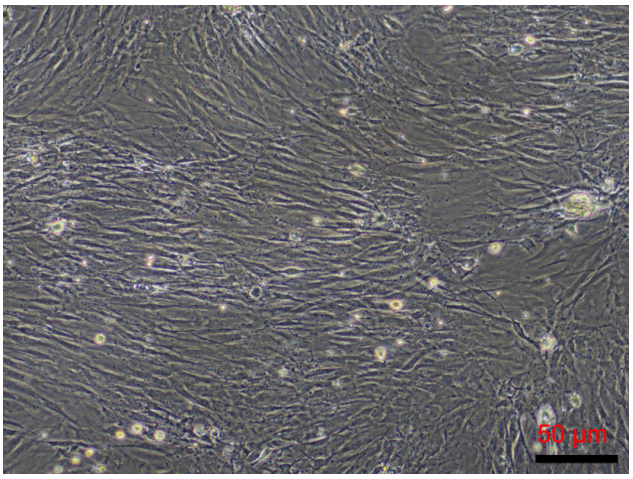

Fig. 1. Cell morphology of the third-generation rat bone marrow mesenchymal stem cells (BMSCs). Scale bars: 50 μm. Original magnification, 100×.

Lipogenic Induction and Oil Red O Staining

After confirming the uniformity and viability of BMSCs, we progressed to explore their adipogenic differentiation potential, a fundamental aspect to validate their multipotency. This differentiation was critical to discern the flexibility and adaptability of the stem cells in varying developmental pathways. Post-induction with adipogenic medium, observations revealed slight cellular enlargement. On the seventh day of induction, transparent lipid droplets began appearing in the cytoplasm. Over time, these droplets increased in size and coalesced, and by the 28th day, they were distinctly stained red by oil red O, confirming a positive lipogenic induction (Fig. 2).

BMSCs Osteogenic Induction and Modified Alizarin Red S Staining

Exploring BMSCs' osteogenic differentiation was critical to gain comprehensive insights into their potential role in bone regeneration therapies. A morphological alteration from long spindle to polygonal shape post osteogenic induction was observed without notable alterations in cell size. From the ninth day onwards, the appearance of calcium salt deposits within the cytoplasm was visible. A subsequent modified alizarin red S staining at two weeks post-induction highlighted the presence of calcium salt deposits, establishing positive osteogenic differentiation (Fig. 3).

Nissel Staining after Noggin Induction of BMSCs

Noggin's role in inducing BMSCs transformation was crucial to comprehend, given its inhibitory effect on bone morphogenetic protein (BMP) signaling. Our focus was to monitor the morphological changes post-induction closely. For some rat BMSCs, after 1 hour of Noggin induction, the cytoplasm was retracted, the refractivity around the nucleus was enhanced, the cell morphology changed from a

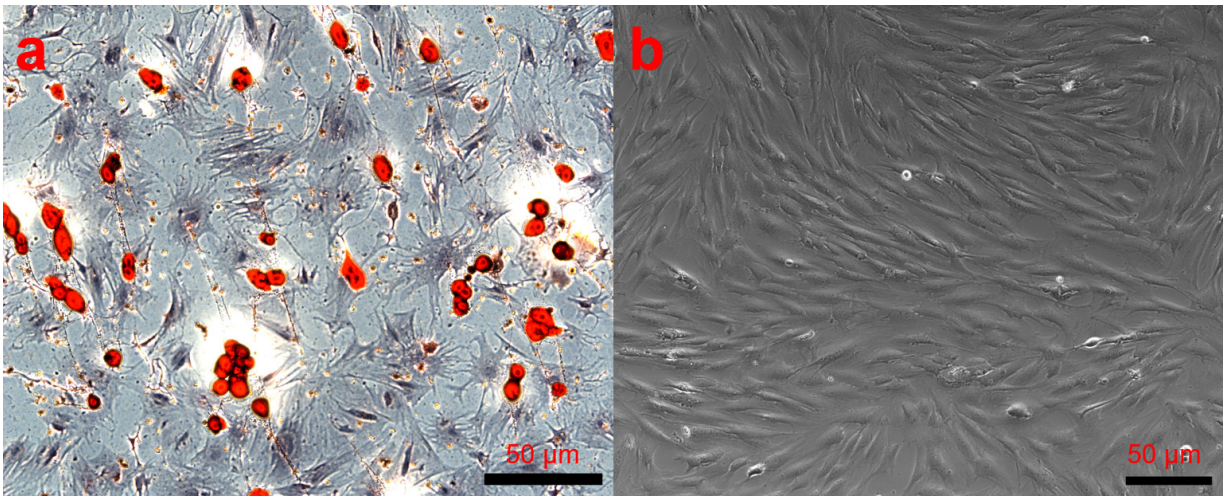

Fig. 2. Oil red O staining post-lipogenic induction. Scale bars: 50 μm. Original magnification, 100×. (a) Oil red O staining after induction of BMSCs into adipocytes. (b) Oil red O staining of the uninduced control group.

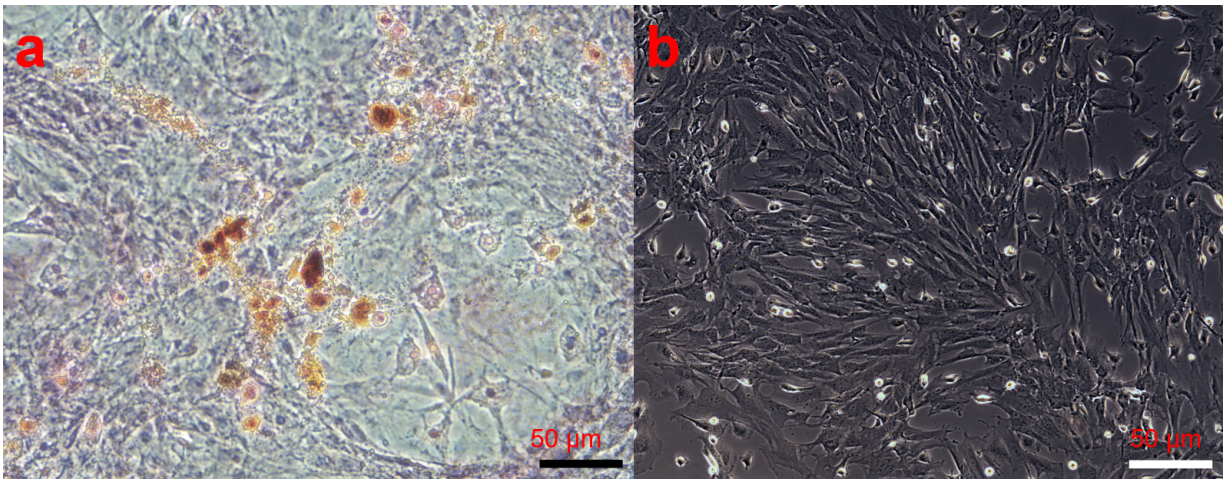

Fig. 3. Modified alizarin red S staining post-osteogenic induction. Scale bars: 50 μm. Original magnification, 100×. (a) Modified alizarin red S staining after osteoblast induction of BMSCs. (b) Modified alizarin red S staining of the uninduced control group.

long spindle to a round shape, and synapses were protruding from the periphery of some cells; After 2 hour of induction, the refractivity was further enhanced, the length of the protrusions increased, and some protrusions overlapped and cross-linked each other, the secondary branches were observed in a small number of protrusions, having the similar shape with neuronal cells (Fig. 4a,b), which were called neuron-like cells, followed by gradual neuron-like cells death. The uninduced control group showed no significant changes in cell morphology and negative Nissel staining (Fig. 4c). The organelle fragments remaining after cell death were visible in the microscope field at about 6 hours. The staining positive rate of each concentration group at each time point was compared, and the result showed that the induction rate of the 75 ng/mL group at 2 h was 0.64 $\pm$ 0.03, significantly higher than the other concentration groups at each time point, with statistically significant differences ($p < 0.05$) (Fig. 5a,b).

Immunofluorescent Detection of SYN1, NF200, and GFAP Expression Post 75 ng/mL Noggin Induction

Understanding the expression levels of various neuronal and glial markers post-Noggin induction is fundamental for elucidating the potential neurogenic differentiation of BMSCs. Neuron-like cells, after 75 ng/mL Noggin induction, were analyzed via immunofluorescence to assess the expression of NF200, SYN1, and GFAP protein expression. The observation of positive expressions (Fig. 6a,b), primarily in the cytoplasm and formation of protrusions, correlated with the induced cell morphological changes, further highlighting the induction's effectiveness in neuronal differentiation. However, we also observed a lack of GFAP expression (Fig. 6c).

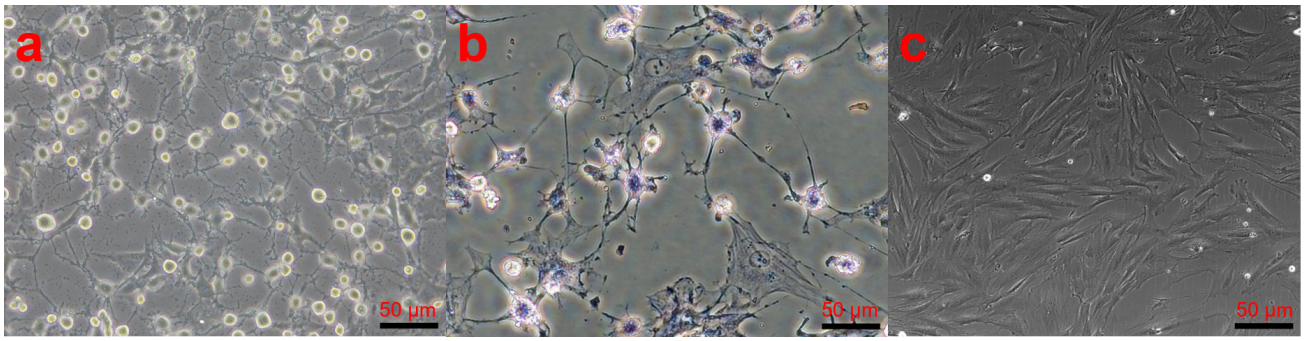

Fig. 4. Nissel staining results of Noggin-induced BMSCs. Scale bars: 50 μm. Original magnification, 100×. (a) Cell morphology of rat BMSCs induced by Noggin. (b) Niseel staining results of cells induced by Noggin, positive result with purple coloration of cells in the result of Nissel staining. (c) Nissel staining of the uninduced control group.

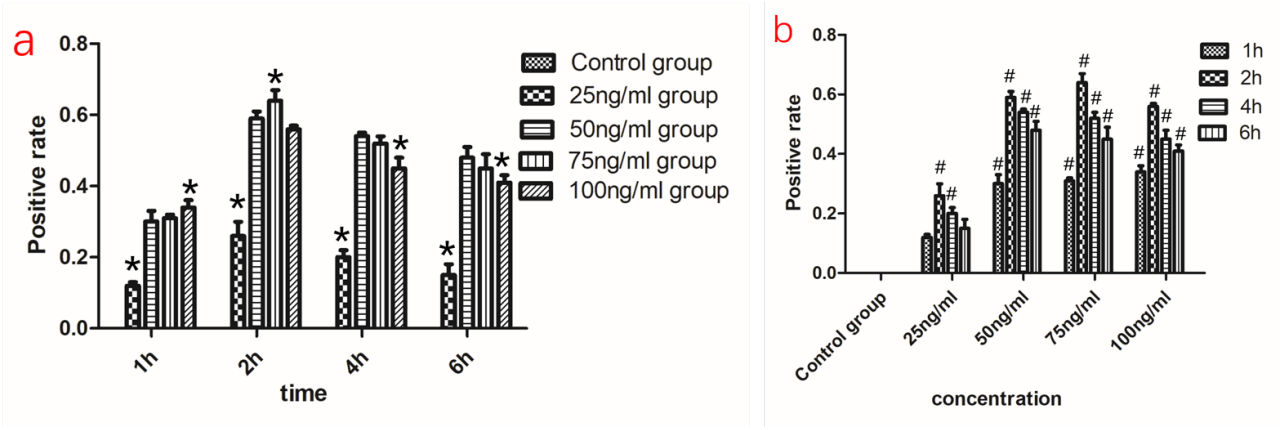

Fig. 5. Nissel staining positive rate of cells in different time points and concentration groups. (a) Nissel staining positive rate of cells in each concentration group at different time points. (b) Nissel staining positive rate of cells at each time point in each concentration group. * and # means $p < 0.05$, vs. control group (mean ± SD, n = 5; One-way analysis of variance and Newman-Keuls multiple comparison test).

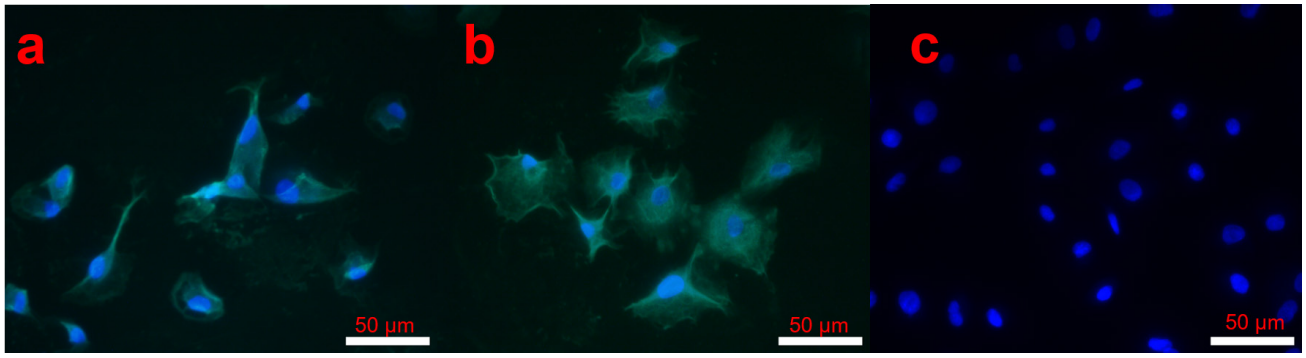

Fig. 6. Neurofilament protein 200 (NF200), synaptic protein I (SYN1), and glial fibrillary acidic protein (GFAP) expression in induced cells (immunofluorescence). Scale bars: 50 μm. Original magnification, 200×. (a) Induced cells positively express NF200. (b) Induced cells positively express SYN1. (c) Induced cells negatively express GFAP. Blue: nucleus staining; Green: target protein (NF200, SYN1, GFAP) staining.

Recovery of Hindlimb Motor Function Post Neuron Induction in SCI Rats

Evaluating the potential therapeutic implications of Noggin-induced neurons required the investigation of motor function recovery in spinal cord injury (SCI) rats. The Basso, Beattie, and Bresnahan (BBB) scores were utilized as a standard measure to document the progression of motor function restoration in SCI rats, offering an in-depth view

of the rehabilitative trajectory. The BBB scores showed significant improvement between 12 h and 4 weeks post-restoration compared to the control group, reaching 9.25 ± 0.63 at week 4 ($p < 0.05$) (Fig. 7).

NF200 mRNA Levels in Local Spinal Cord Tissue Post Neuron Induction

To further expand our understanding of the long-term consequences and integration of neuron-like cells in spinal cord tissues, we conducted a detailed analysis of NF200 mRNA relative expression within the local spinal cord tissue. We aimed to shed light on the molecular mechanisms and the overarching implications of utilizing Noggin-induced neurons for spinal cord repairs, thereby offering a more detailed view of these induced neurons' long-term impacts and adaptability within the spinal cord tissue environment.

The expression of NF200 mRNA in the local spinal cord tissue of the control group gradually decreased over time; In the neuron-like cell group, the expression of NF200 mRNA in the local spinal cord tissue gradually decreased within 1 week, and gradually stabilized after 1 week. When we analyzed the expression levels, the neuron-like group at the 12-hour modeling displayed an NF200 mRNA expression at 3.15 ± 0.37, substantially higher than the control group at 0.38 ± 0.02. A similar trend was observed at various time points, with the expression levels in the neuron-like group surpassing those in the control group (Fig. 8). This molecular profile reinforced the transformative role of Noggin-induced neurons, illustrating their presence and consistent mRNA expression, thereby validating their significant contribution to neural resilience and recovery post spinal cord injury. The pronounced expression of NF200 mRNA in the neuron-like cell group at each analyzed time point was notably higher compared to the control group. This difference was statistically significant ($p < 0.05$), underscoring the potential of induced neurons in advancing spinal cord injury therapeutics.

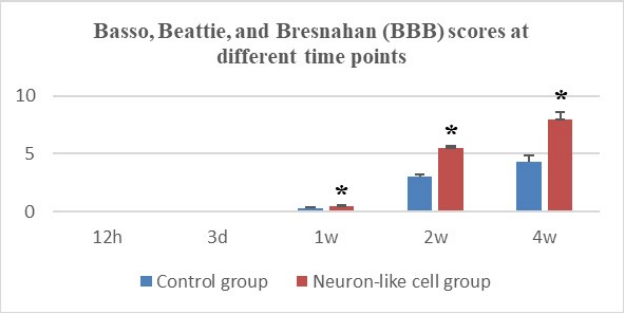

Fig. 7. BBB scores at different time points. $^{*}p < 0.05$, vs. control group (mean ± SD, n = 3; Independent Samples *t*-test).

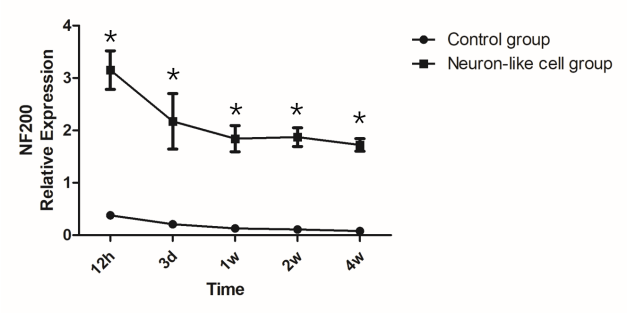

Fig. 8. Relative expression of NF200 mRNA at different time points post neuron-like cell repair in rat spinal cord injury (SCI) tissue ($^{*}p < 0.05$, vs. control group; n = 3; Independent Samples *t*-test).

Discussion

Addressing spinal cord injury (SCI) is a critical focal point within the global healthcare and research community, emphasized by its high incidence and significant socio-economic impacts, especially in young to middle-aged populations [12]. The predominance of SCI in under-40 individuals accentuates the urgency to develop innovative and effective therapeutic interventions, rendering it a pivotal research field in spinal surgery and neurosurgery. Existing treatments for SCI, including spinal decompression surgery and glucocorticoid drugs, predominantly address secondary consequences such as edema and inflammation. However, these interventions fall short of replenishing the loss of neuronal cells and axonal connections, which are fundamental to the pathology of SCI [13]. This underscores the rapid need for strategies to replenish neurons post-SCI within neurosurgery and nerve regeneration research.

Bone marrow mesenchymal stem cells (BMSCs) have emerged as promising tools in neural regeneration research due to their potential to differentiate across germ layers, coupled with their accessibility and absence of ethical controversy [14]. The identification of Noggin, isolated in 1992 by Harland and William Smith of the University of California, and its widespread involvement in developmental processes of the nervous system, and other physiological systems, laid a foundation for exploring its potential in promoting neural restoration [15,16].

Moreover, recent studies have uncovered the synergistic relationship between Noggin and the neural differentiation of BMSCs, with Noggin effectively inhibiting the osteogenic effects of BMP2/4, thereby potentially facilitating the development of the nervous system [17–20]. In light of these findings, our study was designed to leverage Noggin in inducing BMSCs into neurons and investigate their consequential roles in promoting recovery in a rat model of SCI.

In this study, the whole bone marrow adherent method was used to isolate and culture BMSCs, shaped like long shuttles, aggregated and developed in a fishtail pattern, consistent with the typical morphology of rat BMSCs. The outcomes of both lipogenic and osteogenic inductions were positive, reflecting the multidirectional differentiation potential of the obtained BMSCs. Microscopic observation of morphological changes in rat BMSCs induced by Noggin protein, revealed that after 1 hour of induction, some cells exhibited refractivity and formed protrusions, resembling neuron cells morphologically. As induction progressed, the protrusions lengthened, with some developing secondary branches resembling neuron-like cells. Nissel staining, specific for neurons, was conducted at each concentration and time point, determining 75 ng/mL as the optimal Noggin concentration and 2 hours as the optimal induction time.

Immunofluorescence was applied to assess the expression of SYN1, NF200, and GFAP proteins in cells obtained post-induction. The results indicated positive expression of SYN1 and NF200 in the neuron-like cells, with no observed GFAP expression. NF200, predominantly located in neuronal cytoplasm and axons, is crucial for maintaining neuronal morphology, repair, and axonal transport [21]. SYN1 is an important synaptic density and function marker, mainly distributed in the presynaptic membrane and involved in neurotransmitter release [22]. GFAP is an essential astrocyte marker, and its expression reflects astrocyte proliferation [23].

The results highlighted an increase in NF200 protein expression in neuron-like cells derived from rat BMSCs post-Noggin induction, illustrating not only morphological alterations but also molecular changes and the positive expression of neuron-specific markers in rat BMSCs. However, the mere expression of neuron-specific markers doesn't confirm the cellular identity of neurons. Neurons' principal function, neurotransmission, is integral to synapses. Therefore, the induction of neuron-like cells was assessed for synapse formation, revealing positive SYN1 expression. This indicates that the induced cells were analogous to neuron cells in morphology marker expression and had formed complete synapses capable of neurotransmission. The unchanged GFAP expression in induced neuron-like cells denotes Noggin's inability to induce BMSC differentiation into astrocytes, showing a degree of inducibility control.

A rat SCI model was established, and neuron-like cells obtained from Noggin-inducing rat BMSCs were transplanted to the spinal cord injury site. BBB score suggested a gradual recovery in the motor function of the hindlimbs post-transplantation, indicating the cells' therapeutic potential in spinal cord injuries. Further exploration of NF200 mRNA expression in the injured spinal cord illustrated its decreasing trend in both control and neuron-like groups.

SCI occurs in two stages [24]. The first stage is the immediate injury caused by mechanical factors or other pathogens. In this context, it involved scalpel incisions during rat SCI modeling. The subsequent stage is characterized by secondary injury, where the spinal cord tissue experiences disrupted local blood circulation. The production of reactive oxygen, nitric oxide, and free fatty acids is neurotoxic, inducing prolonged damage to the local neurons and axons [25,26]. Therefore, in the control group, the diminishing NF200 mRNA content is attributed to the ongoing death of local neurons due to secondary injuries. Our findings align with the pathological alterations observed in spinal cord injuries.

In contrast, the neuron-like group experienced a decrease in NF200 mRNA expression within the first week post-SCI. This is presumably due to the altered microenvironment at the injury site differing significantly from the *in vitro* culture conditions, causing early-stage damage to the transplanted neuron-like cells by localized free radicals and other environmental factors. However, the expression of NF200 mRNA in the neuron-like group stabilized after 1 week. We speculate that this stabilization is due to the transplanted neuron-like cells changing the local microenvironment, neutralizing local free radicals, and fostering local microcirculation, thus aiding the survival of neurons. Consistently, the BBB score showed gradual recovery in the neuron-like group after 1 week, aligning with the time point of NF200 mRNA stabilization.

Conclusions

In conclusion, we have demonstrated that Noggin can induce the differentiation of rat BMSCs into neuron-like cells *in vitro*. When transplanted into spinal cord injuries, these induced cells facilitate the recuperation of hindlimb motor function in rats. The speculated mode of action is twofold: Firstly, the transplanted neurons form synaptic connects with peripheral neurons, thus re-establishing neural pathways; Secondly, the neuron-like cells enhance the repair of local microcirculation and change the local microenvironment, thereby fostering axonal repair. Future studies are required to understand better the various indicators related to synapse formation and axonal restoration and reveal the specific mechanisms underpinning these observed effects.

Availability of Data and Materials

The data and materials used to support the findings of this study are available from the corresponding author upon request.

Author Contributions

GB, WL and FL designed the research study. GB and WL performed the research. HL assisted with the animal part of the experiment. HW completed the statistical analysis of the experimental data. All authors contributed to ed-

itorial changes in the manuscript. All authors read and approved the final manuscript. All authors have participated sufficiently in the work and agreed to be accountable for all aspects of the work.

Ethics Approval and Consent to Participate

All animal-related operations were approved by the approval of the Experimental Animal Ethics Committee of Zhejiang University School of Medicine, the approval number is ZJU20230311.

Acknowledgment

Not applicable.

Funding

This article is supported by the scientific research project of the Zhejiang Provincial Department of Education (G19014).

Conflict of Interest

The authors declare no conflict of interest.

References

[1] Jiang XH, Li HF, Chen ML, Zhang YX, Chen HB, Chen RH, *et al*. Treadmill exercise exerts a synergistic effect with bone marrow mesenchymal stem cell-derived exosomes on neuronal apoptosis and synaptic-axonal remodeling. Neural Regeneration Research. 2023; 18: 1293–1299.

[2] Davletshin E, Sabirov D, Rizvanov A, Mukhamedshina Y. Combined Approaches Leading to Synergistic Therapeutic Effects in Spinal Cord Injury: State of the Art. Frontiers in Bioscience (Landmark Edition). 2022; 27: 334.

[3] Li Y, Tong Chien W, Sze Ki Cheung D, Wang S, Qin J, Bressington D. Culturally Sensitive Psychosocial Care Program for Chinese People with Spinal Cord Injury During Inpatient Rehabilitation. Alpha Psychiatry. 2022; 23: 140–141.

[4] Zhang X, Liu CB, Yang DG, Qin C, Dong XC, Li DP, *et al*. Dynamic changes in intramedullary pressure 72 hours after spinal cord injury. Neural Regeneration Research. 2019; 14: 886–895.

[5] Lavrov I, Islamov R. Implementing Principles of Neuroontogenesis and Neuroplasticity for Spinal Cord Injury Therapy. Frontiers in Bioscience (Landmark Edition). 2022; 27: 163.

[6] Chaudhari LR, Kawale AA, Desai SS, Kashte SB, Joshi MG. Pathophysiology of Spinal Cord Injury and Tissue Engineering Approach for Its Neuronal Regeneration: Current Status and Future Prospects. Advances in Experimental Medicine and Biology. 2023; 1409: 51–81.

[7] Liu X, Jia X. Neuroprotection of Stem Cells Against Ischemic Brain Injury: From Bench to Clinic. Translational Stroke Research. 2023. (online ahead of print)

[8] Al-Sammarraie N, Mahmood M, Ray SK. Neuroprotective role of Noggin in spinal cord injury. Neural Regeneration Research. 2023; 18: 492–496.

[9] Farrukh F, Davies E, Berry M, Logan A, Ahmed Z. BMP4/Smad1 Signalling Promotes Spinal Dorsal Column Axon Regeneration and Functional Recovery After Injury. Molecular Neurobiology. 2019; 56: 6807–6819.

[10] Liu K, Dong X, Wang Y, Wu X, Dai H. Dopamine-modified chitosan hydrogel for spinal cord injury. Carbohydrate Polymers. 2022; 298: 120047.

[11] Khan FI, Ahmed Z. Experimental Treatments for Spinal Cord Injury: A Systematic Review and Meta-Analysis. Cells. 2022; 11: 3409.

[12] Zipser CM, Cragg JJ, Guest JD, Fehlings MG, Jutzeler CR, Anderson AJ, *et al*. Cell-based and stem-cell-based treatments for spinal cord injury: evidence from clinical trials. The Lancet. Neurology. 2022; 21: 659–670.

[13] Megía García A, Serrano-Muñoz D, Taylor J, Avendaño-Coy J, Gómez-Soriano J. Transcutaneous Spinal Cord Stimulation and Motor Rehabilitation in Spinal Cord Injury: A Systematic Review. Neurorehabilitation and Neural Repair. 2020; 34: 3–12.

[14] Anjum A, Yazid MD, Fauzi Daud M, Idris J, Ng AMH, Selvi Naicker A, *et al*. Spinal Cord Injury: Pathophysiology, Multimolecular Interactions, and Underlying Recovery Mechanisms. International Journal of Molecular Sciences. 2020; 21: 7533.

[15] Eli I, Lerner DP, Ghogawala Z. Acute Traumatic Spinal Cord Injury. Neurologic Clinics. 2021; 39: 471–488.

[16] Liu X, Zhang Y, Wang Y, Qian T. Inflammatory Response to Spinal Cord Injury and Its Treatment. World Neurosurgery. 2021; 155: 19–31.

[17] Díaz-Moreno M, Armenteros T, Gradari S, Hortigüela R, García-Corzo L, Fontán-Lozano Á, *et al*. Noggin rescues age-related stem cell loss in the brain of senescent mice with neurodegenerative pathology. Proceedings of the National Academy of Sciences of the United States of America. 2018; 115: 11625–11630.

[18] Li Z, Yu F, Yu X, Wang S. Potential Molecular Mechanism and Biomarker Investigation for Spinal Cord Injury Based on Bioinformatics Analysis. Journal of Molecular Neuroscience: MN. 2020; 70: 1345–1353.

[19] Khattab HM, Kubota S, Takigawa M, Kuboki T, Sebald W. The BMP-2 mutant L51P: a BMP receptor IA binding-deficient inhibitor of noggin. Journal of Bone and Mineral Metabolism. 2019; 37: 199–205.

[20] Krishnapati LS, Khade S, Trimbake D, Patwardhan R, Nadimpalli SK, Ghaskadbi S. Differential expression of BMP inhibitors gremlin and noggin in Hydra suggests distinct roles during budding and patterning of tentacles. Developmental Dynamics. 2020; 249: 1470–1485.

[21] Kirshblum S, Snider B, Eren F, Guest J. Characterizing Natural Recovery after Traumatic Spinal Cord Injury. Journal of Neurotrauma. 2021; 38: 1267–1284.

[22] Jin LY, Li J, Wang KF, Xia WW, Zhu ZQ, Wang CR, *et al*. Blood-Spinal Cord Barrier in Spinal Cord Injury: A Review. Journal of Neurotrauma. 2021; 38: 1203–1224.

[23] Li C, Wu Z, Zhou L, Shao J, Hu X, Xu W, *et al*. Temporal and spatial cellular and molecular pathological alterations with single-cell resolution in the adult spinal cord after injury. Signal Transduction and Targeted Therapy. 2022; 7: 65.

[24] Quadri SA, Farooqui M, Ikram A, Zafar A, Khan MA, Suriya SS, *et al*. Recent update on basic mechanisms of spinal cord injury. Neurosurgical Review. 2020; 43: 425–441.

[25] Cao Y, Zhu S, Yu B, Yao C. Single-cell RNA sequencing for traumatic spinal cord injury. FASEB Journal: Official Publication of the Federation of American Societies for Experimental Biology. 2022; 36: e22656.

[26] Akram R, Anwar H, Javed MS, Rasul A, Imran A, Malik SA, *et al*. Axonal Regeneration: Underlying Molecular Mechanisms and Potential Therapeutic Targets. Biomedicines. 2022; 10: 3186.